

Determination of  $2\beta_S$  in  $B_S^0 \rightarrow J/\psi K^+ K^-$  decays in the presence of a  $K^+ K^-$  S-wave contribution

This article has been downloaded from IOPscience. Please scroll down to see the full text article.

JHEP09(2009)074

(<http://iopscience.iop.org/1126-6708/2009/09/074>)

[The Table of Contents](#) and [more related content](#) is available

Download details:

IP Address: 80.92.225.132

The article was downloaded on 01/04/2010 at 13:42

Please note that [terms and conditions apply](#).

## Determination of $2\beta_s$ in $B_s^0 \rightarrow J/\psi K^+ K^-$ decays in the presence of a $K^+ K^-$ S-wave contribution

---

Yuehong Xie, Peter Clarke, Greig Cowan and Franz Muheim

*School of Physics and Astronomy, University of Edinburgh,  
Mayfield Road, Edinburgh, EH9 3JZ, U.K.*

*E-mail:* [Yuehong.Xie@cern.ch](mailto:Yuehong.Xie@cern.ch), [peter.clarke@ed.ac.uk](mailto:peter.clarke@ed.ac.uk), [g.cowan@ed.ac.uk](mailto:g.cowan@ed.ac.uk),  
[f.muheim@ed.ac.uk](mailto:f.muheim@ed.ac.uk)

**ABSTRACT:** We present the complete differential decay rates for the process  $B_s^0 \rightarrow J/\psi K^+ K^-$  including S-wave and P-wave angular momentum states for the  $K^+ K^-$  meson pair. We examine the effect of an S-wave component on the determination of the CP violating phase  $2\beta_s$ . Data from the B-factories indicate that an S-wave component of about 10% may be expected in the  $\phi(1020)$  resonance region. We find that if this contribution is ignored in the analysis it could cause a bias in the measured value of  $2\beta_s$  towards zero of the order of 10%. When including the  $K^+ K^-$  S-wave component we observe an increase in the statistical error on  $2\beta_s$  by less than 15%. We also point out the possibility of measuring the sign of  $\cos 2\beta_s$  by using the interference between the  $K^+ K^-$  S-wave and P-wave amplitudes to resolve the strong phase ambiguity. We conclude that the S-wave component can be properly taken into account in the analysis.

**KEYWORDS:** B-Physics, CP violation

**ARXIV EPRINT:** [0908.3627](https://arxiv.org/abs/0908.3627)

---

**Contents**

<b>1</b>	<b>Introduction</b>	<b>1</b>
<b>2</b>	<b>Time-dependent angular distributions in the decay <math>B_s^0 \rightarrow J/\psi K^+ K^-</math> including S-wave contributions</b>	<b>1</b>
<b>3</b>	<b>Measuring <math>2\beta_s</math> in the presence of a <math>K^+ K^-</math> S-wave</b>	<b>4</b>
<b>4</b>	<b>Measuring <math>\cos 2\beta_s</math></b>	<b>6</b>
<b>5</b>	<b>Conclusions</b>	<b>9</b>

---

**1 Introduction**

The decay  $B_s^0 \rightarrow J/\psi\phi$  is a golden channel for the measurement of the  $B_s^0$  mixing phase  $-2\beta_s$  which is a very sensitive probe of new physics. It has been extensively studied [1–8]. In the decay  $B_s^0 \rightarrow J/\psi\phi$ , followed by a two-body decay  $\phi(1020) \rightarrow K^+ K^-$ , the  $K^+ K^-$  meson pair is in an orbital P-wave amplitude. However, in the vicinity of the  $\phi(1020)$  mass, the  $K^+ K^-$  system can have contributions from other partial waves. The same comment holds for the  $K^+ K^-$  system in the decay channels  $B^0 \rightarrow K^+ K^- K_S^0$  and  $D^0 \rightarrow K^+ K^- \pi^0$ . The BaBar experiment showed that in these decays the S-wave and P-wave contributions dominate in the mass range above threshold up to  $1.1 \text{ GeV}/c^2$  [9, 10]. In both cases there is a dominant resonant  $\phi(1020)$  contribution. In addition an S-wave  $f_0(980)$  and a non-resonant contribution are found to be necessary to describe the data. These results motivated us to investigate the effects of a possible S-wave contribution to  $B_s^0 \rightarrow J/\psi K^+ K^-$  in the  $\phi(1020)$  mass region.

In the decay  $B_s^0 \rightarrow J/\psi K^+ K^-$  the  $K^+ K^-$  system can only arise from a  $s\bar{s}$  quark pair while in  $B^0 \rightarrow K^+ K^- K_S^0$  and  $D^0 \rightarrow K^+ K^- \pi^0$  it can have contributions from both  $s\bar{s}$  and  $d\bar{d}$ . This makes it difficult to give a quantitative estimate for the S-wave component. In reference [11] the S-wave  $K^+ K^-$  contribution under the  $\phi(1020)$  peak is estimated to be 5 – 10% for decay modes in which the  $K^+ K^-$  arises from an  $s\bar{s}$  quark pair. In this study we consider an S-wave of similar magnitude and assess its impact on the determination of the weak mixing phase  $-2\beta_s$ .

**2 Time-dependent angular distributions in the decay  $B_s^0 \rightarrow J/\psi K^+ K^-$  including S-wave contributions**

We consider P- and S-wave amplitudes in the decay  $B_s^0 \rightarrow J/\psi K^+ K^-$  where the invariant mass of the  $K^+ K^-$  meson pair is in the  $\phi(1020)$  mass region and the  $J/\psi$  meson decays

into a  $\mu^+\mu^-$  pair. The S-wave contribution can be non-resonant or due to the  $f_0(980)$  resonance<sup>1</sup>. We denote decay amplitudes for the  $B_s^0 \rightarrow J/\psi K^+K^-$  by  $\mathbf{A} = (A_0, A_{||}, A_{\perp}, A_S)$ . Here  $A_0$ ,  $A_{||}$  and  $A_{\perp}$  are the three P-wave amplitudes consistent with the  $K^+K^-$  system decaying via the  $\phi(1020)$  resonance.  $A_S$  is the amplitude for a possible S-wave contribution in the  $K^+K^-$  system. The amplitudes for the conjugate decay  $\bar{B}_s^0 \rightarrow J/\psi K^+K^-$  are denoted by  $\bar{\mathbf{A}} = (\bar{A}_0, \bar{A}_{||}, \bar{A}_{\perp}, \bar{A}_S)$ , which, in the absence of direct CP violation, are related to  $\mathbf{A}$  by  $A_0 = \bar{A}_0$ ,  $A_{||} = \bar{A}_{||}$ ,  $A_{\perp} = -\bar{A}_{\perp}$  and  $A_S = -\bar{A}_S$ . Note that  $A_0$  and  $A_{||}$  are CP-even whereas  $A_{\perp}$  and  $A_S$  are CP-odd. The amplitudes  $(A_0, A_{||}, A_{\perp})$  and the amplitude  $A_S$  may have different dependences on the mass  $m_{K^+K^-}$  of the  $K^+K^-$  system. However, in sufficiently small bins of  $m_{K^+K^-}$ , such as the narrow mass region around the  $\phi(1020)$  resonance, the dependences of the amplitudes on  $m_{K^+K^-}$  can be neglected.

We define the total P-wave strength,  $A_P^2 \equiv |A_0|^2 + |A_{||}|^2 + |A_{\perp}|^2$ , the longitudinal and perpendicular polarisation fractions relative to the P-wave strength  $R_{||} \equiv |A_{||}|^2/A_P^2$ , and  $R_{\perp} \equiv |A_{\perp}|^2/A_P^2$ , and the S-wave fraction,  $R_S \equiv |A_S|^2/(A_P^2 + |A_S|^2)$ . The phases of these decay amplitudes are defined by  $A_j = |A_j|e^{i\delta_j}$ , where  $j = 0, ||, \perp, S$ . As only the relative strong phase differences can be measured we adopt the convention  $\delta_0 = 0$ .

An angular analysis is required to disentangle the different CP eigenstates on a statistical basis. The angular observables are denoted as the helicity angles  $\Omega = (\theta_l, \theta_K, \varphi)$ . Here  $\theta_l$  is the angle between the  $\mu^+$  momentum and the direction opposite to the  $B_s^0$  momentum in the  $J/\psi$  rest frame;  $\theta_K$  is the angle between the  $K^+$  momentum and the direction opposite to the  $B_s^0$  momentum in the rest frame of the  $K^+K^-$  system;  $\varphi$  is the angle between the decay planes of the  $J/\psi \rightarrow \mu^+\mu^-$  and the  $K^+K^-$  pair, when going from the positive kaon to the positive lepton with a rotation around the opposite direction of the  $B_s^0$  momentum in the  $J/\psi$  rest frame.

The differential decay rate for a  $B_s^0$  meson produced at time  $t = 0$  decaying as  $B_s^0 \rightarrow J/\psi K^+K^-$  at proper time  $t$  is given by

$$\frac{d^4\Gamma(B_s^0 \rightarrow J/\psi K^+K^-)}{dt d\cos\theta d\cos\psi d\varphi} \propto \sum_{k=1}^{10} h_k(t) f_k(\Omega), \tag{2.1}$$

whereas the differential decay rate for an initial  $\bar{B}_s^0$  meson is given by

$$\frac{d^4\Gamma(\bar{B}_s^0 \rightarrow J/\psi K^+K^-)}{dt d\cos\theta d\cos\psi d\varphi} \propto \sum_{k=1}^{10} \bar{h}_k(t) f_k(\Omega). \tag{2.2}$$

Each of the  $h_k(t)$ ,  $\bar{h}_k(t)$  and  $f_k(\Omega)$  for  $k = 1 - 10$  are defined in table 1. In total there are four amplitude-squared terms for the three polarisations of the P-waves and the S-wave component plus six interference terms.

The time-dependence of the ten functions  $h_k(t)$  for an initial  $B_s^0$  meson state can be

---

<sup>1</sup>The mass dependence of the  $f_0(980)$  is distorted as the central value of the resonance is below threshold.

$k$	$h_k(t)$	$\bar{h}_k(t)$	$f_k(\theta_l, \theta_K, \varphi)$
1	$ A_0(t) ^2$	$ \bar{A}_0(t) ^2$	$4 \sin^2 \theta_l \cos^2 \theta_K$
2	$ A_{\parallel}(t) ^2$	$ \bar{A}_{\parallel}(t) ^2$	$(1 + \cos^2 \theta_l) \sin^2 \theta_K - \sin^2 \theta_l \sin^2 \theta_K \cos 2\varphi$
3	$ A_{\perp}(t) ^2$	$ \bar{A}_{\perp}(t) ^2$	$(1 + \cos^2 \theta_l) \sin^2 \theta_K + \sin^2 \theta_l \sin^2 \theta_K \cos 2\varphi$
4	$\Im\{A_{\parallel}^*(t)A_{\perp}(t)\}$	$\Im\{\bar{A}_{\parallel}^*(t)\bar{A}_{\perp}(t)\}$	$2 \sin^2 \theta_l \sin^2 \theta_K \sin 2\varphi$
5	$\Re\{A_0^*(t)A_{\parallel}(t)\}$	$\Re\{\bar{A}_0^*(t)\bar{A}_{\parallel}(t)\}$	$-\sqrt{2} \sin 2\theta_l \sin 2\theta_K \cos \varphi$
6	$\Im\{A_0^*(t)A_{\perp}(t)\}$	$\Im\{\bar{A}_0^*(t)\bar{A}_{\perp}(t)\}$	$\sqrt{2} \sin 2\theta_l \sin 2\theta_K \sin \varphi$
7	$ A_S(t) ^2$	$ \bar{A}_S(t) ^2$	$\frac{4}{3} \sin^2 \theta_l$
8	$\Re\{A_S^*(t)A_{\parallel}(t)\}$	$\Re\{\bar{A}_S^*(t)\bar{A}_{\parallel}(t)\}$	$-\frac{2}{3}\sqrt{6} \sin 2\theta_l \sin \theta_K \cos \varphi$
9	$\Im\{A_S^*(t)A_{\perp}(t)\}$	$\Im\{\bar{A}_S^*(t)\bar{A}_{\perp}(t)\}$	$\frac{2}{3}\sqrt{6} \sin 2\theta_l \sin \theta_K \sin \varphi$
10	$\Re\{A_S^*(t)A_0(t)\}$	$\Re\{\bar{A}_S^*(t)\bar{A}_0(t)\}$	$\frac{8}{3}\sqrt{3} \sin^2 \theta_l \cos \theta_K$

**Table 1.** Definition of the functions  $h_k(t)$ ,  $\bar{h}_k(t)$  and  $f_k(\theta_l, \theta_K, \varphi)$  of eq. 2.1 and 2.2.

written as:

$$|A_0(t)|^2 = |A_0|^2 e^{-\Gamma_s t} \left[ \cosh\left(\frac{\Delta\Gamma_s t}{2}\right) - \cos \Phi \sinh\left(\frac{\Delta\Gamma_s t}{2}\right) + \sin \Phi \sin(\Delta m_s t) \right], \quad (2.3)$$

$$|A_{\parallel}(t)|^2 = |A_{\parallel}|^2 e^{-\Gamma_s t} \left[ \cosh\left(\frac{\Delta\Gamma_s t}{2}\right) - \cos \Phi \sinh\left(\frac{\Delta\Gamma_s t}{2}\right) + \sin \Phi \sin(\Delta m_s t) \right], \quad (2.4)$$

$$|A_{\perp}(t)|^2 = |A_{\perp}|^2 e^{-\Gamma_s t} \left[ \cosh\left(\frac{\Delta\Gamma_s t}{2}\right) + \cos \Phi \sinh\left(\frac{\Delta\Gamma_s t}{2}\right) - \sin \Phi \sin(\Delta m_s t) \right], \quad (2.5)$$

$$\Im\{A_{\parallel}^*(t)A_{\perp}(t)\} = |A_{\parallel}||A_{\perp}| e^{-\Gamma_s t} \left[ -\cos(\delta_{\perp} - \delta_{\parallel}) \sin \Phi \sinh\left(\frac{\Delta\Gamma_s t}{2}\right) + \sin(\delta_{\perp} - \delta_{\parallel}) \cos(\Delta m_s t) - \cos(\delta_{\perp} - \delta_{\parallel}) \cos \Phi \sin(\Delta m_s t) \right], \quad (2.6)$$

$$\Re\{A_0^*(t)A_{\parallel}(t)\} = |A_0||A_{\parallel}| e^{-\Gamma_s t} \cos(\delta_{\parallel} - \delta_0) \left[ \cosh\left(\frac{\Delta\Gamma_s t}{2}\right) - \cos \Phi \sinh\left(\frac{\Delta\Gamma_s t}{2}\right) + \sin \Phi \sin(\Delta m_s t) \right], \quad (2.7)$$

$$\Im\{A_0^*(t)A_{\perp}(t)\} = |A_0||A_{\perp}| e^{-\Gamma_s t} \left[ -\cos(\delta_{\perp} - \delta_0) \sin \Phi \sinh\left(\frac{\Delta\Gamma_s t}{2}\right) + \sin(\delta_{\perp} - \delta_0) \cos(\Delta m_s t) - \cos(\delta_{\perp} - \delta_0) \cos \Phi \sin(\Delta m_s t) \right], \quad (2.8)$$

$$|A_S(t)|^2 = |A_S|^2 e^{-\Gamma_s t} \left[ \cosh\left(\frac{\Delta\Gamma_s t}{2}\right) + \cos \Phi \sinh\left(\frac{\Delta\Gamma_s t}{2}\right) - \sin \Phi \sin(\Delta m_s t) \right], \quad (2.9)$$

	$\Delta m_s$	$\Gamma_s$	$\Delta\Gamma_s$	$\delta_0$	$\delta_{\parallel}$	$\delta_{\perp}$	$R_{\parallel}$	$R_{\perp}$	$R_S$	$\delta_S$	$2\beta_s$
Input	17.8 ps <sup>-1</sup>	0.68 ps <sup>-1</sup>	0.05 ps <sup>-1</sup>	0	-2.93	2.91	0.207	0.233	vary	vary	vary
Fit	fix	fix	fix	fix	float	float	float	float	float*	float	float

\* $R_S$  is fixed to 0 when the S-wave component is neglected.

**Table 2.** Values of the physical parameters used in the generation of signal decays and how these parameters are treated in the fit.

$$\Re\{A_S^*(t)A_{\parallel}(t)\} = |A_S||A_{\parallel}|e^{-\Gamma_s t} \left[ -\sin(\delta_{\parallel} - \delta_S) \sin \Phi \sinh \left( \frac{\Delta\Gamma_s t}{2} \right) + \cos(\delta_{\parallel} - \delta_S) \cos(\Delta m_s t) - \sin(\delta_{\parallel} - \delta_S) \cos \Phi \sin(\Delta m_s t) \right], \quad (2.10)$$

$$\Im\{A_S^*(t)A_{\perp}(t)\} = |A_S||A_{\perp}|e^{-\Gamma_s t} \sin(\delta_{\perp} - \delta_S) \left[ \cosh \left( \frac{\Delta\Gamma_s t}{2} \right) + \cos \Phi \sinh \left( \frac{\Delta\Gamma_s t}{2} \right) - \sin \Phi \sin(\Delta m_s t) \right], \quad (2.11)$$

$$\Re\{A_S^*(t)A_0(t)\} = |A_S||A_0|e^{-\Gamma_s t} \left[ -\sin(\delta_0 - \delta_S) \sin \Phi \sinh \left( \frac{\Delta\Gamma_s t}{2} \right) + \cos(\delta_0 - \delta_S) \cos(\Delta m_s t) - \sin(\delta_0 - \delta_S) \cos \Phi \sin(\Delta m_s t) \right], \quad (2.12)$$

where  $\Phi = -2\beta_s$ ,  $\Delta m_s$ ,  $\Delta\Gamma_s$  and  $\Gamma_s$  denote the weak mixing phase, mass difference, decay width difference and average decay width of the  $B_s^0$ - $\bar{B}_s^0$  system, respectively. Here we have assumed that each of the decay amplitudes in  $\mathbf{A}$  is dominated by a single weak phase, therefore a common effective  $2\beta_s$  can be used for all CP eigenstates. The time evolution functions  $\bar{h}_k(t)$  for an initial  $\bar{B}_s^0$  meson can be obtained by reversing the sign of each term proportional to  $\sin(\Delta m_s t)$  or  $\cos(\Delta m_s t)$  in  $h_k(t)$ .

### 3 Measuring $2\beta_s$ in the presence of a $K^+K^-$ S-wave

In this section we investigate how the measurement of  $2\beta_s$  is affected by the presence of a possible  $K^+K^-$  S-wave contribution. We use Monte Carlo simulated toy data based on the differential decay rate expressions of section 2. We generate signal decays only and ignore backgrounds underneath the  $B_s^0$  mass peak as well as all detector effects. The inclusion of these effects does not alter the qualitative results of this study.

We assume a tagging efficiency  $\epsilon_{\text{tag}} = 56\%$  and a wrong tag probability  $\omega_{\text{tag}} = 33\%$ , which correspond approximately to the expected flavour tagging performance for this channel at the LHCb experiment [12]. In table 2 we summarize the values of the physical parameters used to generate the toy data sets.

We generate 500 data sets for different scenarios where we vary the values of the S-wave fraction  $R_S$  and its phase  $\delta_S$  and the weak phase  $-2\beta_s$ . Each data set contains 30000 signal events corresponding to approximately one quarter of a nominal LHCb year of  $2\text{ fb}^{-1}$ .

We perform fits to each data set where  $2\beta_s$ ,  $R_S$ ,  $\delta_S$ ,  $R_{\parallel}$ ,  $\delta_{\parallel}$ ,  $R_{\perp}$ ,  $\delta_{\perp}$  are free parameters and all other parameters are kept fixed. We also perform fits where the S-wave component

	Float $R_S$ in fit	Fix $R_S$ to 0 in fit
$R_S = 0$		$\sigma(2\beta_s) = 0.045$ , $\text{Mean}(2\beta_s) = 0.038$
$R_S = 0.1, \delta_S = \pi/2$	$\sigma(2\beta_s) = 0.048$ , $\text{Mean}(2\beta_s) = 0.035$	$\sigma(2\beta_s) = 0.045$ , $\text{Mean}(2\beta_s) = 0.032$
$R_S = 0.1, \delta_S = 0$	$\sigma(2\beta_s) = 0.054$ , $\text{Mean}(2\beta_s) = 0.040$	$\sigma(2\beta_s) = 0.048$ , $\text{Mean}(2\beta_s) = 0.036$
$R_S = 0.05, \delta_S = \pi/2$	$\sigma(2\beta_s) = 0.048$ , $\text{Mean}(2\beta_s) = 0.040$	$\sigma(2\beta_s) = 0.045$ , $\text{Mean}(2\beta_s) = 0.036$
$R_S = 0.05, \delta_S = 0$	$\sigma(2\beta_s) = 0.055$ , $\text{Mean}(2\beta_s) = 0.038$	$\sigma(2\beta_s) = 0.047$ , $\text{Mean}(2\beta_s) = 0.032$

**Table 3.** Statistical errors and mean values of  $2\beta_s$  from 500 fits for different scenarios with  $2\beta_s = 0.0368$ . The errors on  $\sigma(2\beta_s)$  and  $\text{mean}(2\beta_s)$  are approximately 0.003 and 0.002, respectively. The same data sets are used to obtain the results in the second and third columns.

	Float $R_S$ in fit	Fix $R_S$ to 0 in fit
$R_S = 0$		$\sigma(2\beta_s) = 0.044$ , $\text{Mean}(2\beta_s) = 0.198$
$R_S = 0.1, \delta_S = \pi/2$	$\sigma(2\beta_s) = 0.052$ , $\text{Mean}(2\beta_s) = 0.199$	$\sigma(2\beta_s) = 0.047$ , $\text{Mean}(2\beta_s) = 0.166$
$R_S = 0.1, \delta_S = 0$	$\sigma(2\beta_s) = 0.056$ , $\text{Mean}(2\beta_s) = 0.202$	$\sigma(2\beta_s) = 0.049$ , $\text{Mean}(2\beta_s) = 0.170$
$R_S = 0.05, \delta_S = \pi/2$	$\sigma(2\beta_s) = 0.049$ , $\text{Mean}(2\beta_s) = 0.197$	$\sigma(2\beta_s) = 0.048$ , $\text{Mean}(2\beta_s) = 0.182$
$R_S = 0.05, \delta_S = 0$	$\sigma(2\beta_s) = 0.053$ , $\text{Mean}(2\beta_s) = 0.198$	$\sigma(2\beta_s) = 0.048$ , $\text{Mean}(2\beta_s) = 0.180$

**Table 4.** Statistical errors and mean values of  $2\beta_s$  from 500 fits for different scenarios with  $2\beta_s = 0.2$ . The errors on  $\sigma(2\beta_s)$  and  $\text{mean}(2\beta_s)$  are approximately 0.003 and 0.002, respectively. The same data sets are used to obtain the results in the second and third columns.

is present in the generated toy data, but ignored in the fit ( $R_S$  is set to 0) in order to investigate the bias in the determination of  $2\beta_s$ .

The results of these fits for the statistical error and mean value of the weak phase  $-2\beta_s$  are summarized in table 3, 4 and 5 for several different scenarios with  $-2\beta_s = -0.0368$ ,  $-2\beta_s = -0.2$  and  $-2\beta_s = -0.5$ , respectively. As an example, in figure 1 we show the distributions of the fitted values of  $-2\beta_s$  for  $R_S = 0.1, \delta_S = \pi/2$  and  $-2\beta_s = -0.5$  for both the S-wave fraction  $R_S$  fixed to zero and  $R_S$  left free in the fits. In figure 2 we show the distributions of the fitted values of  $R_S$  and the strong phase of the S-wave component  $\delta_S$  for the same case with  $R_S$  left free in the fit. It can be seen that when all parameters are fitted the results are unbiased, but when it is wrongly assumed that  $R_S = 0$ , the result for  $-2\beta_s$  acquires a bias with regard to the true input value.

Figure 3 shows the bias in  $-2\beta_s$  from neglecting an S-wave component with  $R_S = 0.1$  and  $\delta_S = \pi/2$  versus the value of  $-2\beta_s$  used to generate the data sets. A linear dependence is observed, which demonstrates that the bias in  $-2\beta_s$  is proportional to the true value of  $-2\beta_s$ . From tables 3, 4 and 5 we observe biases for these scenarios which range from 7–17% in the measurement of  $2\beta_s$  if an S-wave component is present, but left unaccounted for in the fits. The bias moves the measured value of  $2\beta_s$  towards zero. This implies that the neglected CP-odd S-wave contribution has a bigger probability to be mis-identified as the CP-even longitudinal or parallel components than as the CP-odd perpendicular component. Therefore, although the bias from neglecting an S-wave contribution is unlikely to lead to false signal of new physics, it will cause a loss of sensitivity to new physics. On the other hand, including the S-wave in the fit removes the bias in the central value of  $2\beta_s$  at a cost of an increase of less than 15% in the statistical error.

	Float $R_S$ in fit	Fix $R_S$ to 0 in fit
$R_S = 0$		$\sigma(2\beta_s) = 0.051$ , $\text{Mean}(2\beta_s) = 0.501$
$R_S = 0.1, \delta_S = \pi/2$	$\sigma(2\beta_s) = 0.059$ , $\text{Mean}(2\beta_s) = 0.501$	$\sigma(2\beta_s) = 0.053$ , $\text{Mean}(2\beta_s) = 0.415$
$R_S = 0.1, \delta_S = 0$	$\sigma(2\beta_s) = 0.061$ , $\text{Mean}(2\beta_s) = 0.501$	$\sigma(2\beta_s) = 0.052$ , $\text{Mean}(2\beta_s) = 0.417$
$R_S = 0.05, \delta_S = \pi/2$	$\sigma(2\beta_s) = 0.051$ , $\text{Mean}(2\beta_s) = 0.506$	$\sigma(2\beta_s) = 0.048$ , $\text{Mean}(2\beta_s) = 0.463$
$R_S = 0.05, \delta_S = 0$	$\sigma(2\beta_s) = 0.053$ , $\text{Mean}(2\beta_s) = 0.501$	$\sigma(2\beta_s) = 0.049$ , $\text{Mean}(2\beta_s) = 0.461$

**Table 5.** Statistical errors and mean values of  $2\beta_s$  from 500 fits for different scenarios with  $2\beta_s = 0.5$ . The errors on  $\sigma(2\beta_s)$  and  $\text{mean}(2\beta_s)$  are approximately 0.003 and 0.002, respectively. The same data sets are used to obtain the results in the second and third columns.

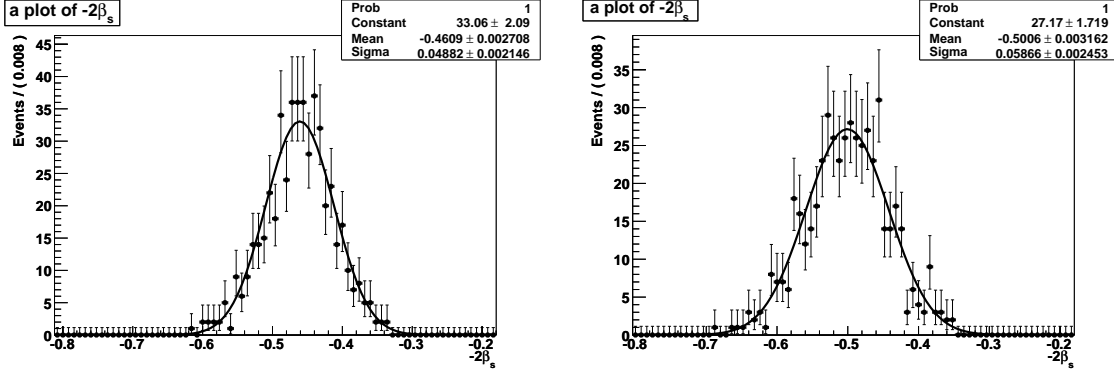


**Figure 1.** Distributions of the fitted values of  $-2\beta_s$  for the scenario  $R_S = 0.1, \delta_S = \pi/2, 2\beta_s = 0.5$ . The left and right plots are obtained with or without fixing  $R_S$  to 0 in fitting the data, respectively.

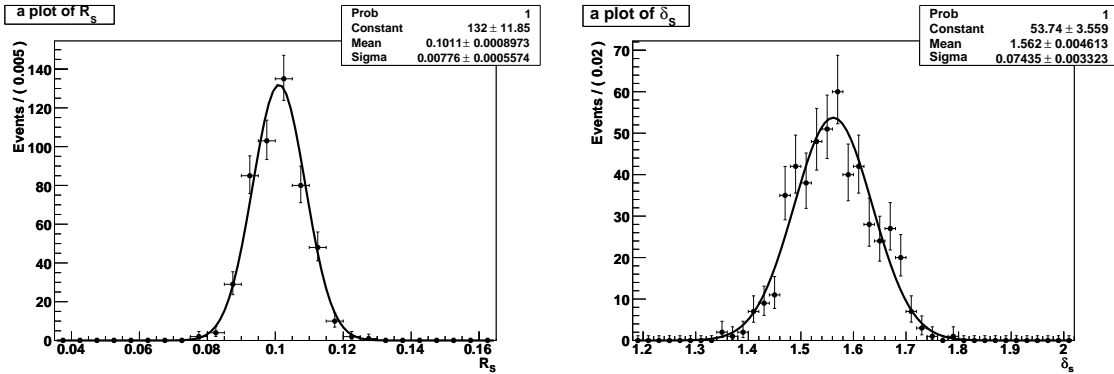


**Figure 2.** Distributions of the fitted values of  $R_S$  and  $\delta_S$  for the scenario  $R_S = 0.1, \delta_S = \pi/2, 2\beta_s = 0.5$  without fixing  $R_S$  to 0 in fitting the data.

#### 4 Measuring $\cos 2\beta_s$

In eq. (2.1) and (2.2) one observes that the differential decay rates are invariant under the transformation

$$(\delta_{\parallel} - \delta_0, \delta_{\perp} - \delta_0, \delta_S - \delta_0, -2\beta_s, \Delta\Gamma_s) \leftrightarrow (\delta_0 - \delta_{\parallel}, \pi + \delta_0 - \delta_{\perp}, \delta_0 - \delta_S, \pi - (-2\beta_s), -\Delta\Gamma_s). \quad (4.1)$$

As a consequence the measurement of  $2\beta_s$  is subject to a two-fold ambiguity, which is



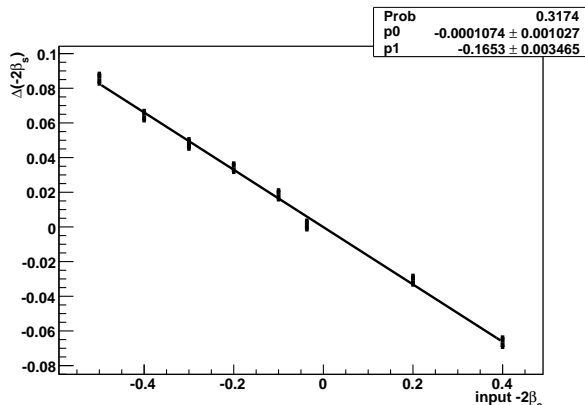


**Figure 3.** The bias in  $-2\beta_s$  from neglecting an S-wave component with  $R_S = 0.1$  and  $\delta_S = \pi/2$  versus the value of  $-2\beta_s$  used to generate the data sets. The bias is the difference of the mean of the fitted to the generated  $-2\beta_s$  values. A linear fit is superimposed on the graph.

equivalent to  $\cos 2\beta_s$  transforming into  $-\cos 2\beta_s$ . A measurement of  $\cos 2\beta_s$  including its sign would allow us to resolve this ambiguity.

If the interference between the P-wave and S-wave amplitudes were to be significant in the  $\phi(1020)$  mass region, we could use this effect to measure  $\cos 2\beta_s$ , in the same way as BaBar measured  $\cos 2\beta$  in  $B^0 \rightarrow J/\psi K_S^0 \pi^0$  [13]. This requires measuring  $\delta_S - \delta_0$ , the strong phase difference between the S-wave and the longitudinal P-wave, as a function of the  $K^+K^-$  mass in the  $\phi(1020)$  mass region. When plotting this function, two branches are expected with each corresponding to a different solution for the weak phase (see figure 4 left). It is straightforward to choose the physical solution since the phase of the P-wave Breit-Wigner amplitude is expected to rise rapidly through the  $\phi(1020)$  mass region (dashed red curve in figure 4 right), while the phase of the S-wave amplitude, which can be described either by a coupled channel Breit-Wigner function in case of an  $f_0$  contribution or by a constant term in case of a non-resonant contribution, is expected to vary relatively slowly (dotted green curve in figure 4 right), resulting in  $\delta_S - \delta_0$  rapidly falling with increasing  $K^+K^-$  mass (solid blue curves in figure 4).

Below we use a Monte Carlo simulated toy data set to demonstrate the feasibility of this method in measuring the sign of  $\cos 2\beta_s$ . We generate 30000  $B_s^0 \rightarrow J/\psi K^+K^-$  events in the  $K^+K^-$  mass region between 1 and 1.05  $\text{GeV}/c^2$ , roughly corresponding to  $0.5 \text{ fb}^{-1}$  of integrated luminosity. The P-wave and  $f_0$  contributions are included coherently. The values of the parameters used to generate the toy data set are the same as in table 2 except that we set  $-2\beta_s = -0.0368$ , and that the values of both  $R_S$  and  $\delta_S$  depend on the  $K^+K^-$  mass. The  $f_0$  contribution accounts for about 10% of the total decay rate in the given mass region, as is shown in figure 5.

The data sample is divided into bins in the  $K^+K^-$  mass. For each bin  $i$ , two parameters  $\delta_{S,i}$  and  $R_{S,i}$  are used to represent the average strong phase and the fraction of the  $f_0$  contribution. Both  $\sin 2\beta_s$  and  $\cos 2\beta_s$  are treated as independent free parameters. Common free parameters  $\sin 2\beta_s$ ,  $\cos 2\beta_s$ ,  $R_{||}$ ,  $R_{\perp}$ ,  $\delta_{||}$ ,  $\delta_{\perp}$ ,  $\Gamma_s$  and  $\Delta\Gamma_s$  are used for all bins. Note that we still adopt the convention  $\delta_0 = 0$  as only the relative phase differences in each bin can

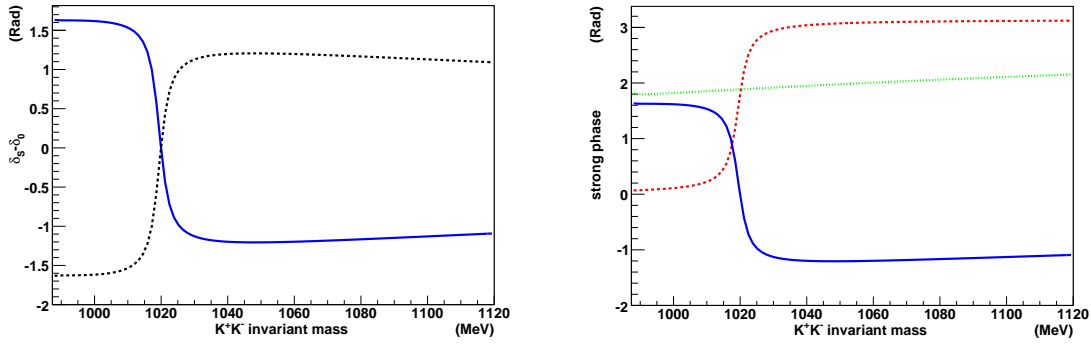


**Figure 4.** An example to illustrate the dependence of the strong phase of the S-wave  $\delta_S$ , of the strong phase of the longitudinal P-wave  $\delta_0$ , and of their difference  $\delta_S - \delta_0$ , on the  $K^+K^-$  mass. Left: the solid blue curve is the physical solution for  $\delta_S - \delta_0$  and the dashed black curve shows the mirror solution. Right: the dashed red, dotted green and solid blue curves are for  $\delta_0$ ,  $\delta_S$ , and  $\delta_S - \delta_0$ , respectively.

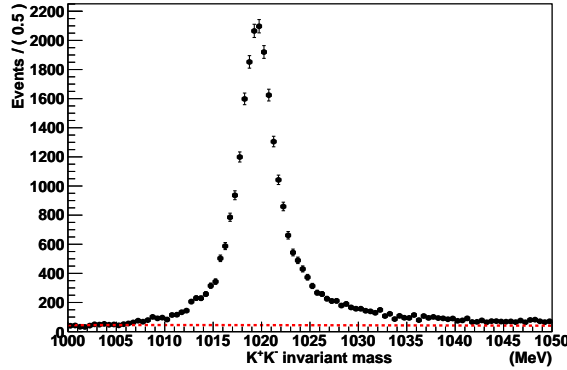


**Figure 5.** The data points correspond to the  $K^+K^-$  mass distribution of a generated sample of  $B_s^0 \rightarrow J/\psi K^+K^-$  events including 10%  $f_0$  contribution in the mass region. The dotted red curve indicates the  $f_0$  contribution.

be measured. A combined fit to the time-dependent angular distributions of all the bins is performed to extract these free parameters. The fitted values of the strong phase difference  $\delta_S - \delta_0$  versus the  $K^+K^-$  mass are plotted in figure 6. The two branches correspond to opposite values of  $\cos 2\beta_s$ . Just as expected, the branch corresponding to the true solution decreases rapidly around the nominal  $\phi(1020)$  mass. Choosing this branch leads to the unique solution

$$\sin 2\beta_s = 0.043 \pm 0.05, \quad \cos 2\beta_s = 1.05 \pm 0.08, \quad (4.2)$$

which gives the ambiguity-free result

$$-2\beta_s = -0.043 \pm 0.05. \quad (4.3)$$

In this example, the measured  $-2\beta_s$  is separated from  $\pi - (-2\beta_s)$  by  $13\sigma$ , therefore the discrete ambiguity in  $2\beta_s$  is completely resolved. Although the actual measurement pre-

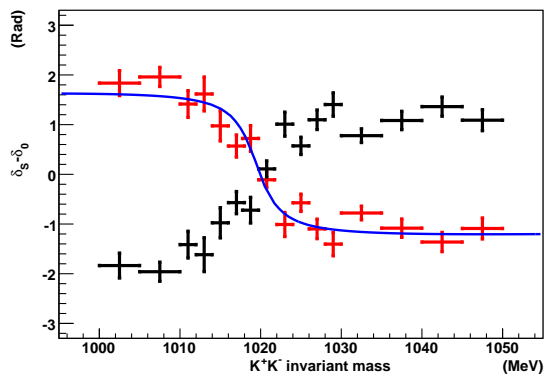


**Figure 6.** The fitted values of  $\delta_S - \delta_0$  versus  $K^+K^-$  mass are shown in red and black data points, corresponding to opposite values of  $\cos 2\beta_s$ . The blue curve shows the dependence of  $\delta_S - \delta_0$  on  $K^+K^-$  mass implemented in simulation.

cision in  $\cos 2\beta_s$  will depend on the size of the  $f_0$  contribution as well as background, the possibility to resolve the ambiguity in  $-2\beta_s$  using this method is very promising.

## 5 Conclusions

In the decay  $B_s^0 \rightarrow J/\psi K^+K^-$  we expect that a  $K^+K^-$  S-wave contribution in the narrow  $\phi(1020)$  mass region could be as large as 10%. The full differential decay rates for this decay including the S-wave contribution have been presented. We have considered a range of scenarios which include S-wave components of 5% and 10%. We have shown that within these scenarios, if an S-wave component is ignored in the analysis, the measurement of the weak phase  $-2\beta_s$  would be biased by between 7% and 17% towards zero. We have demonstrated that by properly allowing for this S-wave component in the fit, an unbiased measurement of  $2\beta_s$  may be obtained with a slightly increased statistical error. Finally, we have shown that the interference between the  $K^+K^-$  S-wave and P-wave amplitudes can be used to resolve the two-fold ambiguity in the measurement of the weak phase  $-2\beta_s$ .

## Acknowledgments

The authors would like to acknowledge the LHCb colleagues for useful and stimulating discussions. We particularly thank Tim Gershon, Olivier Leroy and Guy Wilkinson for valuable suggestions.

## References

- [1] M. Artuso et al., *B, D and K decays*, *Eur. Phys. J. C* **57** (2008) 309 [[arXiv:0801.1833](#)] [[SPIRES](#)].
- [2] P. Ball and R. Fleischer, *Probing new physics through B mixing: status, benchmarks and prospects*, *Eur. Phys. J. C* **48** (2006) 413 [[hep-ph/0604249](#)] [[SPIRES](#)].

- [3] P. Clarke, C. Mclean and A. Osorio-Oliveros, *Sensitivity studies to  $\beta_s$  and  $\Delta\Gamma_s$  using the full  $B_s^0 \rightarrow J/\psi\phi$  angular analysis at the LHCb*, CERN-LHCB-2007-101.
- [4] M. Ciuchini et al., *Next-to-leading order strong interaction corrections to the  $\Delta(F) = 2$  effective hamiltonian in the MSSM*, *JHEP* **09** (2006) 013 [[hep-ph/0606197](#)] [[SPIRES](#)].
- [5] A. Lenz and U. Nierste, *Theoretical update of  $B_s - \bar{B}_s$  mixing*, *JHEP* **06** (2007) 072 [[hep-ph/0612167](#)] [[SPIRES](#)].
- [6] Z. Ligeti, M. Papucci and G. Perez, *Implications of the measurement of the  $B_s^0 - \bar{B}_s^0$  mass difference*, *Phys. Rev. Lett* **97** (2006) 101801 [[hep-ph/0604112](#)] [[SPIRES](#)].
- [7] CDF collaboration, T. Aaltonen et al., *First flavor-tagged determination of bounds on mixing-induced CP-violation in  $B_s^0 \rightarrow J/\psi\phi$  decays*, *Phys. Rev. Lett.* **100** (2008) 161802 [[arXiv:0712.2397](#)] [[SPIRES](#)].
- [8] D0 collaboration, V.M. Abazov et al., *Measurement of  $B_s^0$  mixing parameters from the flavor-tagged decay  $B_s^0 \rightarrow J/\psi\phi$* , *Phys. Rev. Lett.* **101** (2008) 241801 [[arXiv:0802.2255](#)] [[SPIRES](#)].
- [9] BABAR collaboration, B. Aubert et al., *Measurement of CP-violating asymmetries in the  $B^0 \rightarrow K^+K^-K_s^0$  Dalitz plot*, [arXiv:0808.0700](#) [[SPIRES](#)].
- [10] BABAR collaboration, B. Aubert et al., *Amplitude analysis of the decay  $D^0 \rightarrow K^-K^+\pi^0$* , *Phys. Rev. D* **76** (2007) 011102 [[arXiv:0704.3593](#)] [[SPIRES](#)].
- [11] S. Stone and L. Zhang, *S-waves and the measurement of CP-violating phases in  $B_s$  decays*, *Phys. Rev. D* **79** (2009) 074024 [[arXiv:0812.2832](#)] [[SPIRES](#)].
- [12] M. Calvi, O. Leroy and M. Musy, *Flavour tagging algorithms and performances in LHCb*, CERN-LHCB-2007-058 [[SPIRES](#)].
- [13] BABAR collaboration, B. Aubert et al., *Ambiguity-free measurement of  $\cos(2\beta)$ : time-integrated and time-dependent angular analyses of  $B \rightarrow J/\psi K\pi$* , *Phys. Rev. D* **71** (2005) 032005 [[hep-ex/0411016](#)] [[SPIRES](#)].